Joint distribution of local porosity and local tortuosity in sack paper

Matthias Neumann[1], Eduardo Machado Charry[2,3], Peter Leitl[2,4], Ulrich Hirn[2,3], Karin Zojer[2,3] and Volker Schmidt[1].
[1] Institute of Stochastics, Ulm University, Ulm, Germany
[2] Christian Doppler Laboratory for Mass Transport through Paper, Graz University of Technology, Graz, Austria
[3] Institute of Solid State Physics and NAWI, Graz University of Technology, Graz, Austria
[4] bionic surface technologies GmbH, Graz, Austria

Summary

The porosity of paper is a crucial quantity for most applications. Correspondingly, it is highly desirable to study to which extent the porosity of paper influences strongly related properties such as the air permeance, which is one of the key properties of sack paper. In this article, we investigate the local variability of porosity in sack paper as well as the joint distribution of local porosity and local mean geodesic tortuosity. The latter one is an important microstructure characteristic for air permeance since it is a measure for the sinuosity of transport paths through the pore space. For this investigation, we statistically analyze the 3D porous microstructure of sack paper based on tomographic 3D imaging. The values of local porosity and local mean geodesic tortuosity of multiple, non-overlapping cutouts of the considered sample are determined to obtain a distribution of these quantities. Our analysis clearly shows a negative correlation between local porosity and tortuosity. Using a copula approach, we model the joint probability distribution of local porosity and local mean geodesic tortuosity. This model quantifies the porosity-tortuosity correlation and allows, e.g., for a prediction of the conditional distribution of local mean geodesic tortuosities for a given value of local porosity.

Introduction

As for functional materials in general, the microstructure of paper materials has a strong influence on their macroscopic properties. For analyzing microstructures, the combination of 3D imaging and a subsequent image analysis is a powerful tool, as it allows to compute related characteristics, which are not experimentally accessible, see, e.g., Serra, 1982 or Ohser and Schladitz, 2009.

To characterize pore structures in paper-based materials, X-ray computed tomography (µ-CT) has been established as an appropriate method as illustrated for example by Antoine et al., 2002 and Rolland du Roscoat et al., 2005. Such microstructures reconstructed by µ-CT are typically analyzed in terms of global characteristics such as porosity, air permeance, and mean tortuosity. For sack paper, which is used for the packing of powdered goods, air permeance is – besides tensile energy absorption – the main property (Gurnagul et al., 2009) as it enables an efficient de-aeration of bags during filling. Air permeance, in turn, is assumed to depend on the sinuosity of transport paths (Axelsson and Svensson, 2010). Both, porosity as well as the sinuosity of transport paths, also affect macroscopic properties like effective conductivity and permeability (Koivu et al., 2009, Stenzel et al., 2016, Neumann et al., 2019). This sinuosity is quantified by mean geodesic tortuosity (Neumann et al., 2019).

However, since paper-based materials consist of a complex network of fibers, their microstructure characteristics can have large local fluctuations. This heterogeneity is studied in Rolland du Roscoat et al., 2007 and Rolland du Roscoat et al., 2012, where the authors investigate for which sample sizes global characteristics can be reliably computed despite of local fluctuations. It is also highly desirable to quantify the variability between distinct locations itself. In our case, we particularly consider porosity and mean geodesic tortuosity as local characteristics and investigate their local distributions. Rather than considering just the two individual (univariate) distributions, we also investigate the joint (bivariate) distribution of these quantities. In particular, we utilize so-called copulas (Nelsen, 2007) to parametrically model the bivariate distribution of local porosity and local mean geodesic tortuosity. Note that for this investigation of local effects in the pore structure, the focus is on the quantification of the local variability and we do not intend to determine a representative volume element of the paper sheet as in Rolland du Roscoat et al., 2007 and Rolland du Roscoat et al., 2012.

Having fitted the model to the sample, it allows us to (i) quantify the correlation between local porosity and local mean geodesic tortuosity and to (ii) compute the conditional distribution of local mean geodesic tortuosity for given a local porosity. Our results reveal information about the impact of local variability of porosity on local variability of the sinuosity of transport path, and thus on the local air permeance of sack paper.

Material, imaging and data pre-processing for the investigation of local characteristics

We consider the microstructure of sack paper made of unbleached pulp with a specific basis weight of $70\ gm^{-2}$. This type of sack paper is used for the packing of powdered goods, since it exhibits intrinsically a high porosity and a superior mechanical strength. 3D imaging is performed using µ-CT, which leads to an image sample of size $2.0\ mm \times 2.8\ mm$ in xy-plane with cubic voxels having a side length of $1.5\ \mu m$. The images are binarized, i.e. for each voxel, we determine, whether it belongs to cellulose material or to the pore space. For a detailed description of these pre-processing steps leading to the 3D pore structure, visualized in Fig. 1, we refer to Machado Charry et al., 2018, in which a global statistical analysis for this sample is provided. In the following, we denote the direction specifying the paper thickness by z, and the plane orthogonal to z is denoted as the xy-plane.

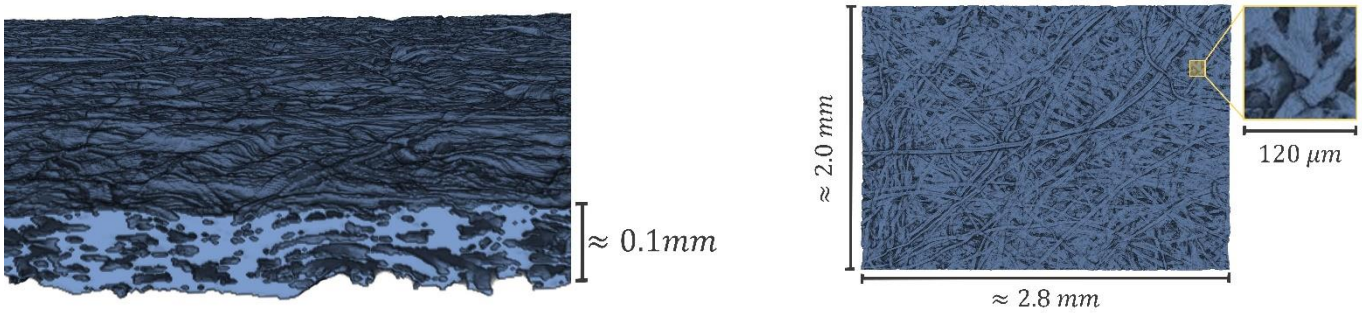

Fig. 1. 3D visualization of the paper sheet reconstructed by µ-CT imaging (left). Top view on the xy-plane of the paper sheet (right) and a zoom to a cutout on the surface of size $120\ \mu m \times 120\ \mu m$.

In order to investigate the local heterogeneity of the 3D microstructure of sack paper, we consider a set of non-overlapping three-dimensional cutouts, which are square-shaped in xy-plane and the centers of the cutouts in xy-plane are arranged on a square grid with a side length of $150\ \mu m$. In z-direction, the complete microstructure of cellulose material is taken into account. This setting leads to a total number of 204 cutouts. The side length of the squares defining the size of cutouts in xy-plane is varied in the range $30\mu m, 60\ \mu m, \dots, 150\ \mu m$. The thickness of cutouts, i.e. the extension in z-direction, is approximately $0.1\ mm$. A cutout of side length $120\ \mu m$ is visualized in Fig. 1 (right panel). The maximum size of the cutouts is chosen such that they do not overlap each other. Note that by considering cutouts with the above mentioned size our focus is on local effects in the microstructure of sack paper, while effects at a larger scale are not taken into account.

We evaluate porosity as well as mean geodesic tortuosity of these cutouts. The mean geodesic tortuosity is defined as the ratio of the expected length of the shortest transport path through the paper sheet (starting at a predefined location at one chosen surface of the sack paper) and the paper thickness. Note that when computing mean geodesic tortuosity for a cutout, we consider all paths the starting points of which are located in the cutout, while the paths themselves are allowed to leave the cutout.

Statistical methods

In this section, we briefly describe the statistical methods which we use to parametrically model the bivariate distribution of local porosity and local mean geodesic tortuosity. The main idea of modeling the bivariate distribution is to use so-called copulas (Nelsen, 2007). This means that we model the univariate – also called marginal – distributions of local porosity and local mean geodesic tortuosity, respectively, at first. In a second step, the joint distribution is modeled under the constraint of given, i.e. the previously determined, marginal distributions.

In the following, we consider local porosity and local mean geodesic tortuosity as random variables, denoted by X and Y, respectively. To model their marginal distributions, we use a beta distribution for X and a generalized gamma distribution for Y. Both distributions are continuous and are thus defined by their probability density functions.

The probability density function of the beta distribution is given by

$$f_X(x) = \frac{\Gamma(p+q)}{\Gamma(p)\Gamma(q)}\, x^{p-1}\,(1-x)^{q-1},$$

for each $x \geq 0$ and $f_X(x) = 0$ for $x < 0$, where $p, q > 0$ are some model parameters and Γ denotes the gamma function. In order to fit the parameters p and q to the observed values of local porosity, we use maximum likelihood estimation as described in Beckman and Tietjen, 1978. The probability density function of the generalized gamma distribution is given by

$$g_Y(y) = \frac{k\, y^{d-1}}{a^d\, \Gamma\left(\frac{d}{k}\right)}\; e^{-\left(\frac{y}{a}\right)^k},$$

for each $y \geq 0$ and $g_Y(y) = 0$ for $y < 0$, where $a, d, k > 0$ are some model parameters. Parameter estimation is performed by maximum likelihood estimation, where the log-likelihood function is maximized by means of the Nelder-Mead algorithm (Nelder and Mead, 1965).

To model the joint distribution of local porosity and local mean geodesic tortuosity, it turns out that the Frank copula (Genest, 1987) is an appropriate model, i.e., we assume that the joint density $h_{X,Y}$ of X and Y is given by

$$h_{X,Y}(x,y) = f_X(x) g_Y(y) \left(\frac{\partial^2 C}{\partial x\, \partial y}\right)\left(\int_0^x f_X(t)\,\mathrm{d}t,\, \int_0^y g_Y(s)\,\mathrm{d}s\right),$$

for each $x, y > 0$ and $h_{X,Y}(x,y) = 0$ otherwise, where

$$C(x,y) = -\frac{1}{\theta}\log\left(1 + \frac{\left(e^{-\theta x}-1\right)\left(e^{-\theta y}-1\right)}{e^{-\theta}-1}\right)$$

and $\theta \in \mathbb{R} \setminus \{0\}$ is a model parameter describing the correlation between local porosity and local mean geodesic tortuosity. The larger the absolute value of θ, the stronger is the correlation, where positive values means positive correlation and vice versa. For quantitative analytical relationships between θ and the correlation measures Kendall's tau and Spearman's rho, we refer to Genest et al., 1995. Note that when modeling the bivariate distribution by means of the density $h_{X,Y}$, the marginal densities of X and Y are given by f_X and g_Y, respectively. Moreover, using this approach, one easily obtains parametric conditional distributions of X and Y. In particular, the conditional distribution of local mean geodesic tortuosity given the local porosity has the density function

$$h_{Y|X=x}(y) = \frac{h_{X,Y}(x,y)}{f_X(x)} = g_Y(y) \left(\frac{\partial^2 C}{\partial x\, \partial y}\right)\left(\int_0^x f_X(t)\,\mathrm{d}t,\, \int_0^y g_Y(s)\,\mathrm{d}s\right),$$

for each x with $f_X(x) > 0$. The parameter θ is determined via pseudo-likelihood estimation as described in Genest et al., 1995.

To enable a comparison of the presented parametric model with the data obtained from image data, we estimate probability density functions based on the observation of discrete data points. For this purpose, kernel density estimation via diffusion (Botev et al., 2010) is used in the univariate as well as in the bivariate case.

Results and Discussion

The marginal distributions of local porosity and local mean geodesic tortuosity estimated from image data for different side lengths of cutouts are visualized in the left panels of Fig. 2. We show the corresponding parametric probability density functions, which are fitted as described in the previous section, in the right panels. The estimated and modeled distributions agree well for both microstructure properties and the general trends are preserved. Firstly, the microstructure properties exhibit a decreasing variability with increasing side lengths of cutouts. Secondly, the distributions of local mean geodesic tortuosity are right-skewed. The skewness is more pronounced for smaller sizes of cutouts.

Table 1. Estimated values and the corresponding standard deviations of the parameter θ describing the correlation between local porosity and local mean geodesic tortuosity.

side length of cutouts	$30\ \mu m$	$60\ \mu m$	$90\ \mu m$	$120\ \mu m$	$150\ \mu m$
estimated value for θ	-2.97 ± 0.50	-3.50 ± 0.52	-4.22 ± 0.54	-4.61 ± 0.55	-4.39 ± 0.55

The values of the parameter θ appearing in the Frank copula correspond to the correlation between local porosity and local mean geodesic tortuosity. The values estimated for each cutout size and the corresponding standard deviations of the estimated values, obtained by Monte-Carlo simulation are given in Table 1. There is a clear negative correlation between the considered microstructure characteristics. The correlation $|\theta|$ increases with cutout size until a side length of 120 μm, while $|\theta|$ decreases slightly upon further increasing the cutout size to 150 μm. The standard deviations of the estimator for θ are between 0.50 and 0.55 for all cutout sizes. Note that these deviations imply that the apparent slight decrease in θ from 120 μm to 150 μm do not necessarily imply a lesser pronounced correlation.

The left panel in Fig. 3 shows the joint distribution of local porosity and local mean geodesic tortuosity estimated from image data for cutouts with a side length of 90 μm. The corresponding joint distribution of the fitted parametric model, right panel in Fig. 3, shows a good visual accordance between model and data. However, the probability density function estimated from image data shows a small peak for local mean geodesic tortuosity larger than 1.5 which we consider as an inaccuracy of the kernel density estimation based on 204 cutouts. Such effects occur more likely when performing kernel density estimation for vector data than for real-valued data (Scott, 2015). Going beyond visual inspection, the model is formally validated by testing the following hypothesis: the values of local porosity and local mean geodesic tortuosity computed from image data follow the same distribution as 204 virtual pairs of local porosity and local mean geodesic tortuosity drawn from the copula model. For this purpose, we use the two sample test proposed in Baringhaus and Franz, 2004. For all cutout sizes, the hypothesis test is not rejected at a significance level of 5 %.

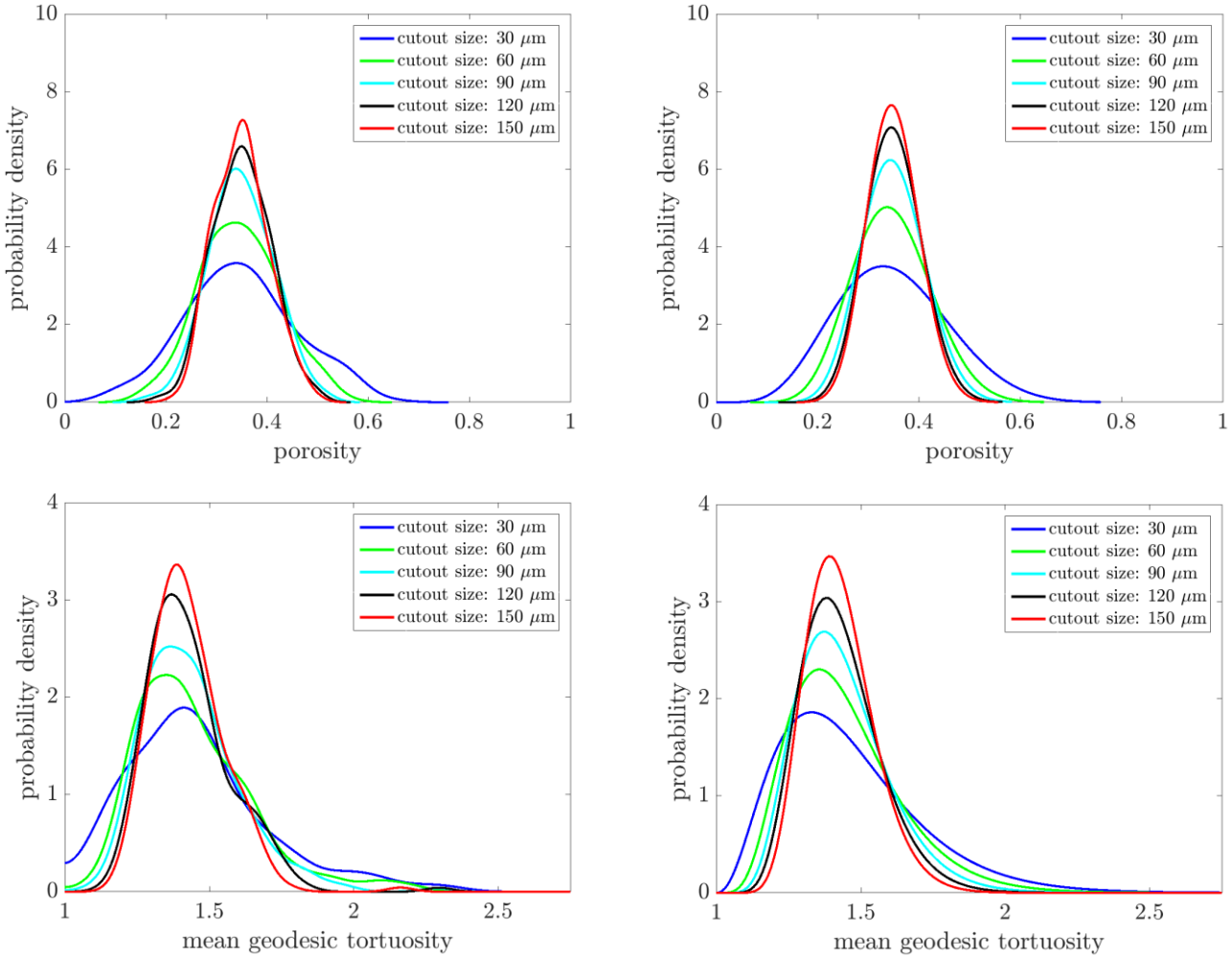

Fig. 2. Distributions of local porosity (top left) and local mean geodesic tortuosity (bottom left) estimated from image data and the corresponding beta (top right) and generalized gamma (bottom right) distributions.

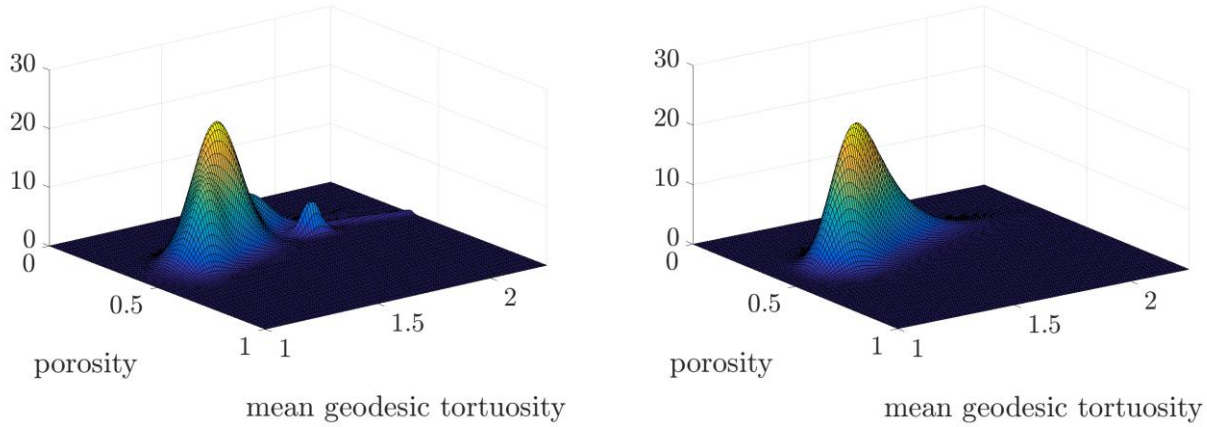

Fig. 3. Joint distribution of local porosity and local mean geodesic tortuosity estimated from image data (left) and of the fitted model (right) for cutouts with a side length of 90 μm.

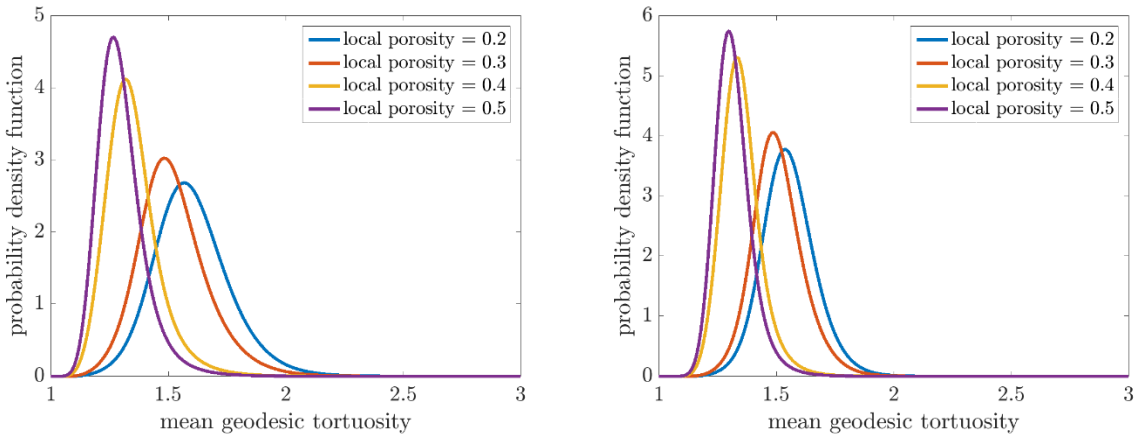

Fig. 4. Conditional distributions of local mean geodesic tortuosities for given local porosities computed by means of the copula model. The side lengths of cutouts are 90 μm (left) and 150 μm (right).

Based on the fitted parametric model for the joint distribution of local porosity and local mean geodesic tortuosity, we compute conditional distributions of local mean geodesic tortuosity for given local porosities. Such conditional distributions, as exemplarily shown in Fig. 4 for cutouts with side lengths of 90 μm and 150 μm, change their shape with increasing porosity. Provided that the local porosity is 0.4 or 0.5, the conditional distributions of local mean geodesic tortuosity are right-skewed, reminiscent to the unconditional distribution of local mean geodesic tortuosity (Fig. 2).

Conclusion

We have parametrically modeled the joint distribution of local porosity and local mean geodesic tortuosity of sack paper, the microstructure of which has been recently investigated with respect to global characteristics in Machado Charry et al., 2018. For this purpose, we have considered cutouts of 3D image data obtained by µ-CT. The parametric model is fitted to different sizes of cutouts. Using the parametric model, which is based on a copula approach, we compute the conditional distribution of local mean geodesic tortuosity given the local porosity of a cutout. Moreover, the model quantifies the negative correlation between both characteristics. Our analysis gives deeper insights regarding the influence of local porosity on the sinuosity of transportation paths through the pore space of sack paper. This is an important step to understand the impact of local porosity on local air permeance – a key property of sack paper.

References

Antoine, C., Nygård, P., Gregersen, Ø. W., Holmstad, R., Weitkamp, T., Rau, C. (2002). 3D images of paper obtained by phase-contrast X-ray microtomography: image quality and binarisation. *Nuclear Instruments and Methods in Physics Research Section A: Accelerators, Spectrometers, Detectors and Associated Equipment*, 490:392–402.

Axelsson, M., Svensson, S. (2010). 3D pore structure characterisation of paper. *Pattern Analysis and Applications*, 13(2):159–172.

Baringhaus, L., Franz, C. (2004). On a new multivariate two-sample test. *Journal of Multivariate Analysis*, 88(1):190–206.

Beckman, R. J., Tietjen, G. L. (1978). Maximum likelihood estimation for the beta distribution. *Journal of Statistical Computation and Simulation*, 7(3-4):253–258.

Botev, Z. I., Grotowski, J. F., Kroese, D. P. (2010). Kernel density estimation via diffusion. *The Annals of Statistics*, 38(5):2916–2957.

Genest, C. (1987). Frank's family of bivariate distributions. *Biometrika*, 74(3):549–555.

Genest, C., Ghoudi, K., Rivest, L.-P. (1995). A semiparametric estimation procedure of dependence parameters in multivariate families of distributions. *Biometrika*, 82(3):543–552.

Gurnagul, N., Shallhorn, P., Omholt, I., Miles, K. (2009). Pressurised high-consistency refining of kraft pulps for improved sack paper properties. *Appita Journal: Journal of the Technical Association of the Australian and New Zealand Pulp and Paper Industry*, 62(1):25.

Koivu, V., Decain, M., Geindreau, C., Mattila, K., Bloch, J.-F., Kataja, M. (2009). Transport properties of heterogeneous materials. Combining computerised X-raymicro-tomography and direct numerical simulations. *International Journal of Computational Fluid Dynamics*, 23(10):713–721.

Machado Charry, E., Neumann, M., Lahti, J., Schennach, R., Schmidt, V., Zojer, K. (2018). Pore space extraction and characterization of sack paper using μ-CT. *Journal of Microscopy*, 272(1):35–46.

Nelder, J. A., Mead, R. (1965). A simplex method for function minimization. *The Computer Journal*, 7:308–313.

Nelsen, R. B. (2007). *An Introduction to Copulas*. Springer, New York.

Neumann, M., Hirsch, C., Staněk, J., Beneš, V., Schmidt, V. (2019). Estimation of geodesic tortuosity and constrictivity in stationary random closed sets. *Scandinavian Journal of Statistics*, in print, https://doi.org/10.1111/sjos.12375.

Neumann, M., Stenzel, O., Willot, F., Holzer, L., Schmidt, V. (2019). Quantifying the influence of microstructure on effective conductivity and permeability: virtual materials testing. *International Journal of Solid and Structures*, in print.

Ohser, J., Schladitz, K. (2009). *3D Images of Materials Structures: Processing and Analysis*. J. Wiley & Sons, Weinheim.

Rolland du Roscoat, S., Decain, M., Thibault, X., Geindreau, C., Bloch, J.-F. (2007). Estimation of microstructural properties from synchrotron X-ray microtomography and determination of the REV in paper materials. *Acta Materialia*, 55(8):2841–2850.

Rolland du Roscoat, S., Bloch, J.-F., Caulet, P. (2012). A method to quantify the 3D microstructure of fibrous materials containing mineral fillers using X-ray microtomography: application to paper materials. *Journal of Materials Science*, 47(18):6517–6521.

Rolland du Roscoat, S., Bloch, J. F., and Thibault, X. (2005). Synchrotron radiation microtomography applied to investigation of paper. *Journal of Physics D: Applied Physics*, 38(10A):A78.

Scott, D. W. (2015). *Multivariate Density Estimation: Theory, Practice, and Visualization*. J. Wiley & Sons, Hoboken.

Serra, J. (1982). *Image Analysis and Mathematical Morphology*. Academic Press, London.

Stenzel, O., Pecho, O. M., Holzer, L., Neumann, M., Schmidt, V. (2016). Predicting effective conductivities based on geometric microstructure characteristics. *AIChE Journal*, 62:1834–1843.